MULTISTATIC SEARCH THEORY

Alan Washburn, Naval Postgraduate School

Mümtaz Karataş, Turkish Naval Academy

ABSTRACT

The characterizing feature of multistatic sensor systems is the inclusion of geographically independent receivers that might receive echoes from any source. We develop a simple analytic theory to predict detection probability, and use it to study pattern optimization, cost/effectiveness, reliability and the relative attractiveness of multistatic versus monostatic systems.

INTRODUCTION

A typical monostatic radar or sonar sensor includes one transmitter or source (Tx) and one receiver (Rx). Tx emits pulses that travel to a target and are reflected from it. Rx detects the reflected pulses, and the time difference between transmission and reception determines the distance to the target. Tx and Rx are co-located, and may even use the same antenna. The range ρ of the sensor is the largest distance at which detection is possible. At its simplest, barring complications due to topography or directional background noise, one can visualize the effect of each sensor as a covered circle with radius ρ. Much of our intuition about search is built on this idea of individual covered areas. For example

1. A barrier can be constructed by using multiple sensors whose circles slightly overlap.
2. The area covered by a system of sensors is easily illustrated on a map.
3. If you move one sensor, there is no effect on the others.

A multistatic system incorporates multiple sources and receivers that are not paired. Any Rx can receive reflected transmissions from any Tx, and they can be present in different numbers. Figure 1 illustrates the basic structure of a monostatic sensor and a multistatic system.

Here are some arguments in favor of multistatic sonar systems:

1. Receivers are less expensive than sources (Amanipour & Olfat, 2011), so it makes sense to employ more receivers than sources. For example, the U.S. Navy's SSQ-125 active sonobuoy costs about five times as much as the SSQ-53 passive sonobuoy, one of the sonobuoy types that can listen for its signals (Signal Online, 2012; USN, 2014).
2. A multistatic system can employ different platforms for sources and receivers. A ship might be Tx, while Rx is a sonobuoy.
3. Sources reveal their locations when they transmit, and targets can use that information to avoid detection. However, the independent receivers in a multistatic system do not reveal their positions.

4. It is possible that the reflected signal will be received by multiple receivers. The resulting location estimate will be more precise, and the phenomenon can also help to eliminate some of the false alarms that monostatic active systems are prey to. We will not deal with these issues in this paper, but Coon (1997) and Ozols & Fewell (2011) discuss the fusion of detections from multiple receivers.

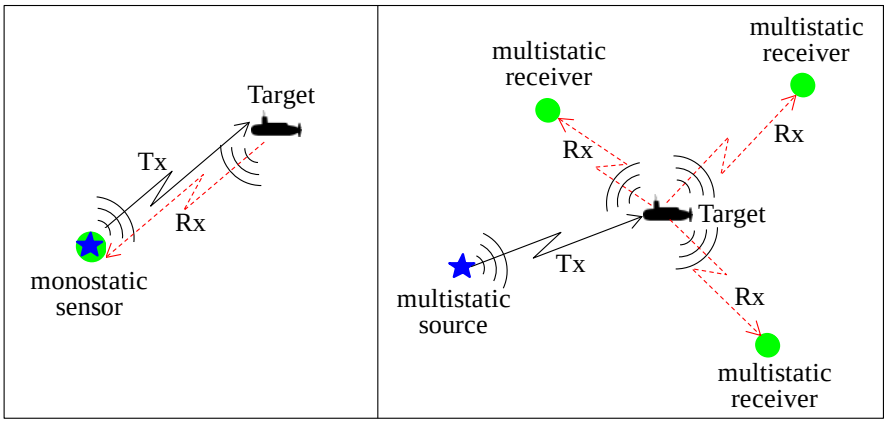

Figure 1. Left: A monostatic sensor with a co-located source and receiver. Right: A multistatic system with one source and three independent receivers.

In spite of the advantages of multistatic systems, there are still circumstances where monostatic systems will perform better. Our interest here is in developing a multistatic theory that is sufficiently simple to enable studies of cost/effectiveness and logistics, including comparisons with monostatic systems. Our motivation comes primarily from underwater detection systems where the targets are submarines, so we will often refer to sources as sonars and receivers as sonobuoys, even though the mathematics is equally applicable to radars or geolocation systems.

Previous studies of multistatic systems focus on issues such as tracking and data fusion (Coraluppi, 2005; Bradaric, et al, 2006; Martina & Frank, 2010; Ozols, et al, 2011; Daun, et al, 2012; Stinco, et al, 2013), localization (Paolini, et al, 2008; Simakov, 2008), imaging (Devaney, 2005; Xie, et al, 2006; Wang, et al, 2012; Ammari, et al, 2012), ping scheduling (Saksena & Wang, 2008; Krout, et al, 2009) and performance prediction & sensor placement (Krieger, et al, 2003; Chacko & DelBalzo, 2007; Tharmarasa, et al, 2009; Ozols & Fewell, 2011; Gong, et al, 2013). There are several currently existing software systems that deal with multistatic sonobuoy fields, including ASPECT, a U.S.Navy tactical decision aid that is capable of predicting detection probability. ASPECT considers geometric optimization questions, and employs a physical model that is more realistic than anything that will be employed here. However, ASPECT is a menu-driven Monte Carlo simulation that is not analytically suitable for considering resource allocation questions. ASPECT is based on the Multistatic Acoustic Simulation Model (MSASM, Bowen & Mitnick (1999)). Other multistatic models described by Bowen & Mitnick include the Multistatic Performance Prediction Methodology (MPPM), where sources are arranged on a rectangular grid, the Sonar Equation Modeling and Simulation Tool (SE-MAST), the Surveillance Operational Concepts Model (SOCM) and the Multistatic Tactical Planning Aid (MSTPA, see also

Wathelet, et al, 2008). All of these models are more realistic and less tractable than the ones considered here.

Our model of detection ignores all of the phenomena that make transmission loss dependent on direction. We assume that the transmission loss at a distance R is proportional to $R^{-\alpha}$ for some positive value of α. Spherical spreading corresponds to $\alpha = 2$, but other values of α will reasonably model most direct-path situations. If R_1 and R_2 are the distances of a source and a receiver from the target, then the total transmission loss is $t = (R_1^{-\alpha})(R_2^{-\alpha}) = (R_1 R_2)^{-\alpha}$, so detection will depend on whether the product $R_1 R_2$ is smaller than some threshold. The detection threshold depends on the source level, the target strength, the sensitivity of the receiver, and the background noise level, all of which can be combined into a single "detection range" ρ with dimensions of length such that detection happens if and only if $R_1 R_2 \le \rho^2$ (see Figure 2, Right). This single-parameter model of detection will be applied throughout.

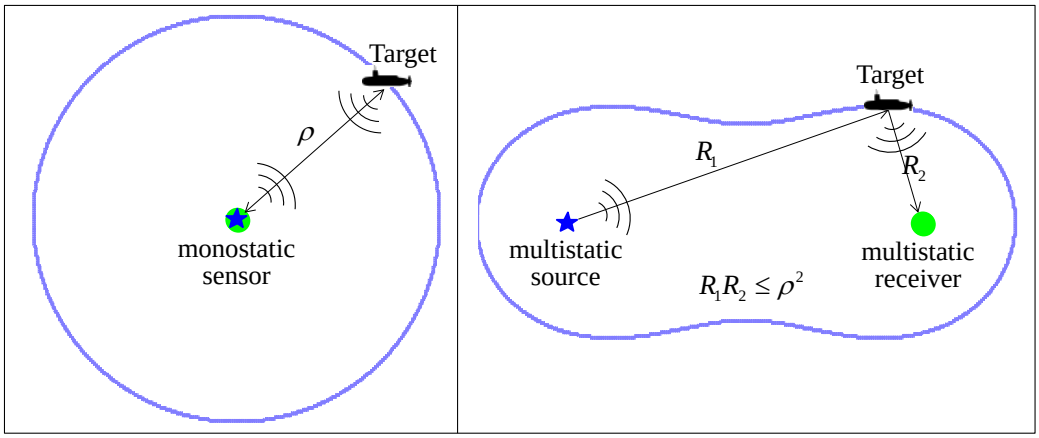

Figure 2. Left: Monostatic sensor with a circular detection region of radius ρ. Right: Multistatic system with a single source and receiver.

Randomly placed fields are analyzed in the next section. Such fields have the simplest summary formulas for effectiveness. Subsequent sections study optimal multistatic sensor geometries, the effectivenesss of mobile sources, cost/effectiveness, reliability and the effects of direct blast.

RANDOMLY PLACED MULTISTATIC FIELDS

Detection Probability

Detection turns out to be easiest to study when both sources and receivers are randomly placed within some large region or "field". Our model of "randomly placed field" will throughout this section be a Poisson field, a generalization of a Poisson process (Feller, 1950). A Poisson field of points in two-dimensional Euclidean space is characterized by a single parameter λ representing the average number of points per unit area. Poisson fields have many desirable analytic properties, one of which is that the number of points inside any region with area V is a Poisson random variable with mean λV. In particular, the probability of finding zero points inside such a region is $\exp(-\lambda V)$,

a fact that will be frequently employed below. We will also use two additional properties:

1. The superposition of a Poisson field with density λ on an independent Poisson field with density μ is a Poisson field with density λ + μ.
2. If a Poisson field with density λ is "thinned" by removing each of its points independently with probability *p*, then the remaining points constitute a Poisson field with density λ(1–*p*).

Consider, then, two independent, two-dimensional Poisson fields, one (sources) with density *g* and the other (receivers) with density *h*. Each source emits an omnidirectional sound that is reflected by a target, and the reflected energy is eventually received by each receiver. If R_1 and R_2 are the distances of a source and a receiver from the target, then detection by that pair happens if and only if $R_1 R_2 \le \rho^2$. Only the smallest such product need concern us, since detection by any source-receiver pair is sufficient for our purposes. We intend to quantify *Q*, the probability that the smallest range product is larger than ρ^2. The nondetection probability is *Q*, and $1 - Q$ is the detection probability.

The two crucial tail functions of interest are $P(R_1 > r) = \exp(-\pi g r^2)$ and $P(R_2 > r) = \exp(-\pi h r^2)$, for all $r \ge 0$. In each case, the event that the nearest distance is larger than *r* is the same as the event that there are no points in a circle with radius *r*; that is, we are employing the formula for the probability that a Poisson random variable is zero. Let $f_{R_2}(r)$ be the probability density function of R_2. This density function is the negative derivative of $P(R_2 > r)$. Since R_1 and R_2 are independent, we have

$$Q = \int_0^\infty P(R_1 > \frac{\rho^2}{r}) f_{R_2}(r) dr = \int_0^\infty \exp(-\frac{\pi g \rho^4}{r^2}) 2\pi h r \exp(-\pi h r^2) dr \,. \qquad (1)$$

Let $s = \pi g \rho^2$ and $t = \pi h \rho^2$ be dimensionless versions of the source and receiver densities, and let $x = \pi h r^2$. Substituting *x*, *s*, and *t* into (1), with $y = 2\sqrt{st}$, we have

$$Q = \int_0^\infty \exp(-(\frac{st}{x} + x)) dx = \int_0^\infty \exp(-(\frac{y^2}{4x} + x)) dx = y K_1(y) \,, \qquad (2)$$

where $K_1(y)$ is a modified Bessel function of order 1 (Abramovitz & Stegun,1964). The detection probability is then

$$P(y) = 1 - Q = 1 - y K_1(y) \,. \qquad (3)$$

The detection probability depends only on the "effort density" parameter *y*, which incorporates all factors of tactical relevance. Figure 3 shows *P*(*y*) together with two approximations, one of which is accurate for small *y* and the other for large *y*. The two approximations are

$$P(y) \approx -\frac{y^2}{2} \ln(\frac{y}{2}) \text{ for small } y, \text{ and } P(y) \approx 1 - \sqrt{\frac{\pi y}{2}} \exp(-y)(1 + \frac{3}{8y}) \text{ for large } y \qquad (4)$$

Both approximations are taken from Abramovitz & Stegun (1964).

Now suppose that x_1 sources and x_2 receivers are randomly placed inside a region of area *A*′, with none outside of *A*′, and that *A*′ is immersed in a larger region *A*

wherein a target is placed at random. We wish to choose A' to maximize the probability that the target is detected. For monostatic systems, the best choice of A' is to make it as large as possible (nearly all of A), since doing so makes it unlikely that the regions covered by the individual sensors will wastefully overlap. This is not necessarily true with multistatic systems because $P(y)$ is not a concave function when y is small, as is evident in Figure 3.

We assume that the target will not be detected if its position lies outside of A', and that a target inside of A' essentially faces two Poisson fields with densities $g = x_1/A'$ and $h = x_2/A'$. The word "essentially" is carefully chosen, since the numbers of buoys within A' would be random in a Poisson field, rather than the fixed numbers x_1 and x_2, but there should be little difference in effectiveness when those numbers are much larger than 1. The first assumption is pessimistic, since targets outside of A' can still be detected, and the second is optimistic, since targets inside of A' do not face complete Poisson fields. Perhaps the two assumptions taken together are neutral, at least if A' is large. The validity of these assumptions will be tested below. Our purpose here is simply to explore the consequences of making both assumptions.

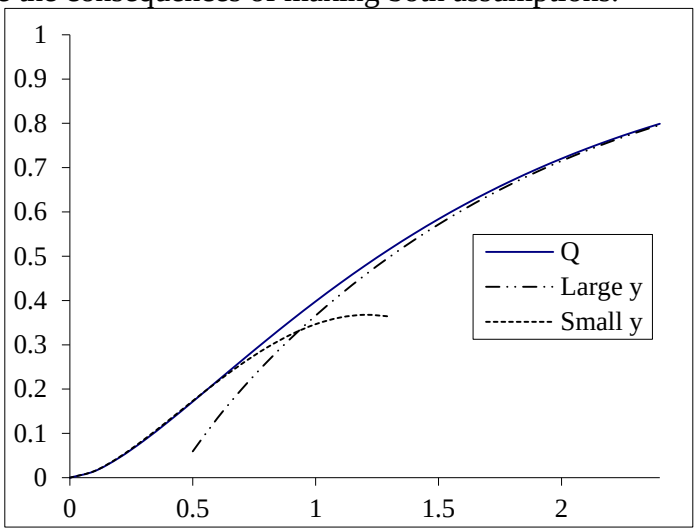

Figure 3. The detection probability *P*(*y*), together with two approximations.

The probability that the target is located in A' is A'/A, and within A' the product of the two densities is $gh = x_1 x_2 /(A')^2$, so the effort parameter within A' is $y' = \dfrac{2\pi\rho^2\sqrt{x_1 x_2}}{A'}$, which determines the conditional detection probability. The searcher can have a large y' in a small area or a small y' in a large area, and must decide which is best. The unconditional detection probability is

$$PD = \frac{A'}{A} P(y') = \frac{2\pi\rho^2\sqrt{x_1 x_2}}{A} \frac{P(y')}{y'} \equiv y \frac{P(y')}{y'} \tag{5}$$

where the last equality defines y. The searcher's problem is to maximize the ratio of $P(y')$ to y', except that y' must be at least y because A' cannot exceed A. Figure 4 shows a graph of the ratio. The maximizing y' is about 1.1 and the maximized ratio is almost exactly 0.4. If y is larger than 1.1, the planner can do no better than to set y' to y

Accounting for this, the maximized *PD* can be obtained from (5). Letting the optimized detection probability be $PD^*(y)$, we have

$$PD^*(y) \equiv \begin{cases} 0.4y; \ y \le 1.1 \\ P(y); \ y \ge 1.1 \end{cases}. \tag{6}$$

Example: Suppose that ρ = 1 km, and that the area to be searched is $A = 200$ km^2. Assume that $x_1 = 20$ sources and $x_2 = 40$ receivers, so that $y = 0.89$. Then the detection probability according to (6) is $PD^*(0.89) = 0.36$, which is achieved by placing all buoys in a fractional (0.89/1.1) part of *A*. If the buoys were mistakenly spread over all of A, the detection probability would be only $P(0.89) = 0.35$, a slight decrease. If the number of receivers is increased to 160, then *y* doubles to 1.78, so the buoys should now be spread over all of *A*. The associated detection probability is $PD^*(1.78) = 0.67$.

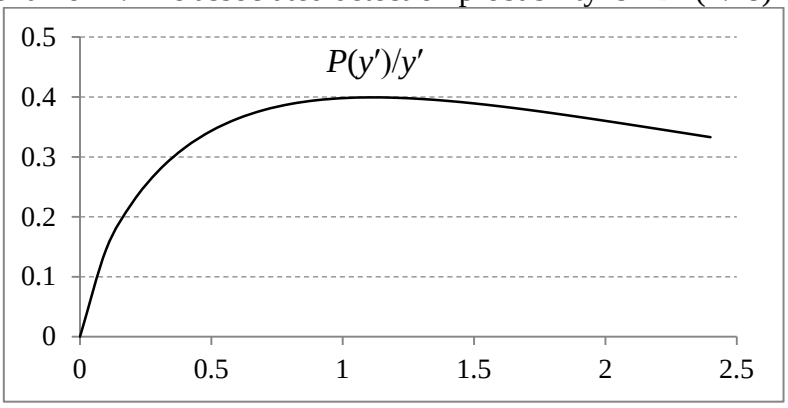

Figure 4. A graph of *P*(*y*′)/ *y*′, the detection probability per unit of effort.

Equivalent Covered Area

A pattern of buoys establishes a probability of detection for a target at point (*x*,*y*), whether that point is inside or outside of the area within which the buoys are deployed. When integrated over the whole plane, that detection function becomes what might be called an "equivalent covered area" (*C*), with equivalency in the sense that, if a target is uniformly distributed over a region with area *A* that is much larger than *C*, then the detection probability is *C*/*A*. The question of maximizing *C* arises. For monostatic buoys, the question is not interesting because the best sonobuoy field (ignoring practical questions about the construction and monitoring of widespread fields) would spread out over all of *A*. With multistatic buoys, however, the question is legitimate. The same argument as above leads to the conclusion that the effort density in the covered part of an optimal field will be about 1.1, and that the resulting equivalent area covered will be

$$C = (0.4)2\pi\rho^2\sqrt{x_1 x_2} \tag{7}$$

Formula (7) is a very simple way of summarizing the effectiveness of a multistatic sonobuoy field. It will later be the basis of a cost/effectiveness analysis.

Neutrality verification

Here we test the neutrality assumption lying behind (5) and (7) by Monte Carlo simulation. Figure 5 shows one replication of randomly placing $x_1 = 4$ sources and $x_2 = 10$ receivers within *A*′, a region that is itself contained within a larger region *A*. The

covered area is all of the area within A that is included in one of the pictured regions, and can be estimated by randomly locating many targets within A (+ signs in the figure) and testing whether each of them is detected. The neutrality assumption is that targets detected outside of A' will compensate for targets inside of A' that are not detected. The assumption is clearly optimistic if A and A' are equal, since in that case there are no targets outside of A'. It is just as clearly pessimistic if buoys are very dense within A', since in that case all targets outside of A' that are within ρ of A' will be detected, in addition to all targets inside of A'. The truth of the neutrality assumption must evidently depend on the density of buoys and the relationship between A and A'.

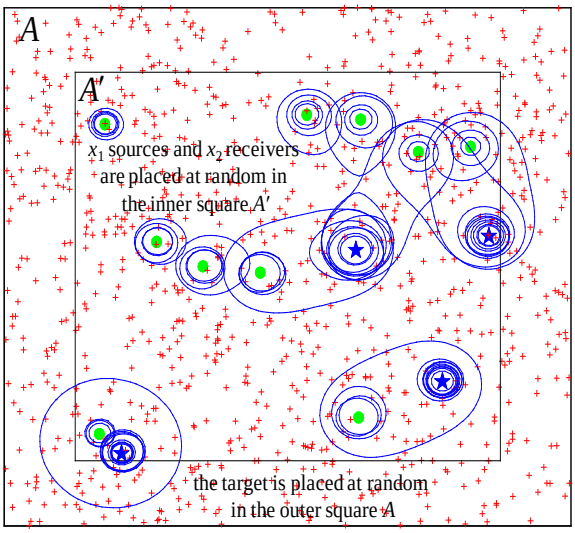

Figure 5. One replication of a simulation experiment to measure covered area. Receivers are marked with • , sources are marked with a star, and targets are marked with a + sign. All targets that lie within some oval are detected.

When area A is large compared to A', we can compare the theoretical equivalent covered area C from (7) with an experimental version C_{exp}. To estimate C_{exp}, without loss of generality we take ρ =1. We also take $A' = 2\pi\sqrt{x_1 x_2}\,/1.1$, since this is the area that theoretically maximizes the covered area. All buoys are placed within a square of side L with area A', so L^2=A'. Detection is impossible for targets more than 1 unit away from this square, so we generate 30 targets at random within a square of side L+2 (so $A = (L+2)^2$), and count the number X that are detected. This experiment is repeated 3,000 times; that is, all the buoys are randomly relocated in A' and each such pattern is tested against 30 targets randomly located in A. Let X be the total number of targets detected in all 3,000 replications. Then the equivalent covered area is $C_{\text{exp}} = AX\,/\,90,000$.

Table 1 shows the ratio C_{exp}/C for various values of x_1 and x_2. The neutrality assumption can be seen to be optimistic, but only by a small amount, with little dependence on x_1 or x_2. The average of all 100 ratios is 96.6%, so the theoretical area coverage is about 3% high. Some idea of the variability of results can be obtained by comparing symmetric entries (x_1,x_2) and (x_2,x_1), since both have the same theoretical mean. For additional tests of the neutrality assumption see Washburn (2010).

Number of Sources (x_1)	Number of Receivers (x_2)										
	5	***10***	***15***	***20***	***25***	***30***	***35***	***40***	***45***	***50***	**AVG**
5	0.960	0.948	0.954	0.953	0.963	0.955	0.954	0.962	0.950	0.954	**0.955**
10	0.966	0.971	0.964	0.964	0.957	0.968	0.956	0.961	0.962	0.956	**0.963**
15	0.957	0.955	0.955	0.968	0.978	0.963	0.963	0.963	0.965	0.974	**0.964**
20	0.954	0.969	0.967	0.965	0.971	0.964	0.956	0.972	0.961	0.965	**0.964**
25	0.955	0.968	0.957	0.965	0.972	0.977	0.970	0.971	0.978	0.962	**0.968**
30	0.948	0.968	0.962	0.969	0.969	0.972	0.984	0.969	0.969	0.971	**0.968**
35	0.958	0.966	0.966	0.966	0.973	0.974	0.967	0.973	0.979	0.976	**0.970**
40	0.965	0.974	0.962	0.970	0.972	0.973	0.971	0.985	0.967	0.971	**0.971**
45	0.951	0.966	0.975	0.961	0.974	0.979	0.967	0.965	0.977	0.977	**0.969**
50	0.960	0.958	0.973	0.970	0.971	0.972	0.982	0.974	0.975	0.972	**0.971**
AVG	**0.957**	**0.964**	**0.964**	**0.965**	**0.970**	**0.970**	**0.967**	**0.970**	**0.968**	**0.968**	**0.966**

Table 1. The table entries are the ratio C_{exp}/C, the ratio of experimental to theoretical equivalent covered area.

OPTIMAL MULTISTATIC SENSOR GEOMETRIES

The beauty of analysis in randomly placed fields is the simplicity of formulas such as (6) for detection probability and (7) for equivalent covered area. However, there is clearly no point in deliberately strewing sensors about at random; it is surely possible to achieve better coverage by deploying sources and receivers in carefully chosen patterns. In this section we investigate the effectiveness of such patterns, one of the goals being to enable comparisons with the random theory.

Cassini Ovals

The boundary of a region where $R_1 R_2 \le \rho^2$ is a Cassini oval (Cox, 1989). If the sensors are fixed at $(\pm a, 0)$, yielding a separation distance of 2*a*, and if (*x*,*y*) is a point on the boundary of the oval, then we must have:

$$\left[(x-a)^2 + y^2\right]\left[(x+a)^2 + y^2\right] = \rho^4, \quad a, \rho \in \mathbb{R}. \tag{8}$$

The boundary is symmetric with respect to both axes, and its shape depends on the dimensionless separation parameter, a/ρ. The form of the ovals can be characterized as follows:

- For $a/\rho \le \sqrt{2}/2$ the curve is a single loop that looks like an ellipse and intersects the *x*-axis at $x = \pm\sqrt{a^2 + \rho^2}$.
- For $\sqrt{2}/2 < a/\rho < 1$ the oval attains a dent on top and bottom.
- When $a/\rho = 1$ the curve is a lemniscate.
- For $a/\rho > 1$ the curve splits into two ovals and there are two additional real *x*-intercepts at $x = \pm\sqrt{a^2 - \rho^2}$.

Figure 6 illustrates the ovals for different values of a/ρ where ρ is fixed at 1. The largest of those ovals in terms of area is the first; with ρ fixed, the area of a Cassini oval is maximized when $a = 0$. Given a single source and a single receiver, the two would therefore best be combined into a single monostatic sonobuoy. However, every source provides a signal for every receiver in a multistatic system, and receivers are usually cheaper than sources. We therefore first investigate the effectiveness of multistatic systems with a single source, but multiple receivers.

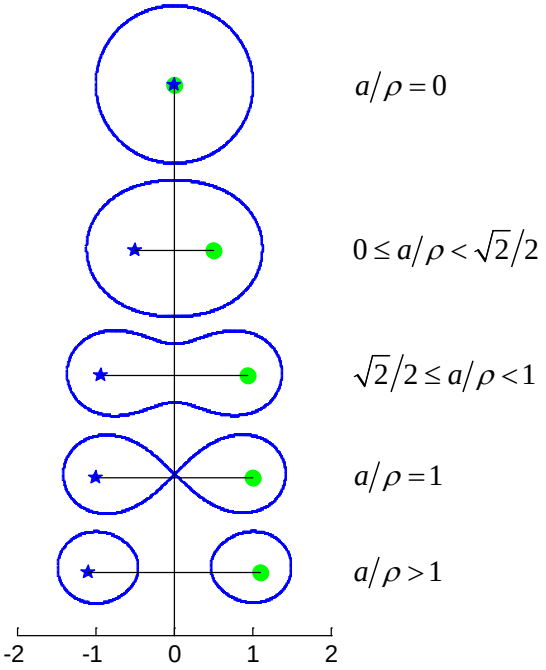

Figure 6. A family of Cassini ovals (ρ=1)

Single Source-Multiple Receivers

We first consider the case where the source is surrounded by a circle of x_2 receivers, experimentally seeking the circle radius a that maximizes the total area covered. Area coverage for each radius is measured by repeated Monte Carlo simulation runs. Figure 7 shows examples of optimal patterns for x_2=3, 6 and 12, stating the optimal radius as a/ρ^*, and giving the corresponding optimized area coverage C.

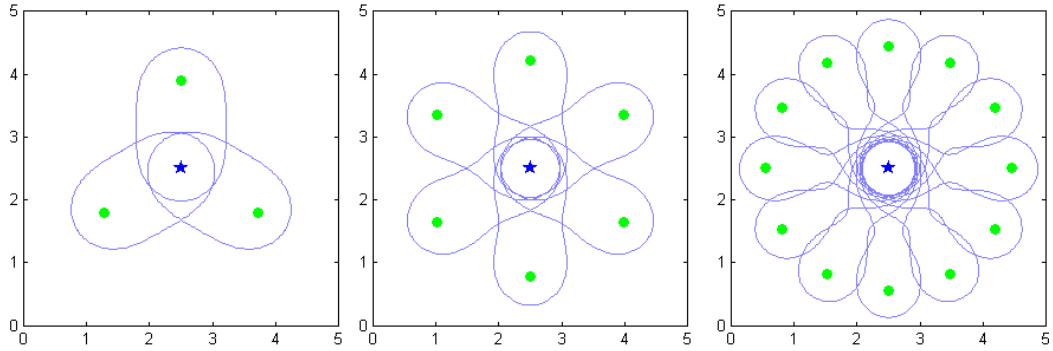

$x_2 = 3$
$a/\rho^* = 0.73$
$C = 6.54\rho^2$

$x_2 = 6$
$a/\rho^* = 0.85$
$C = 10.51\rho^2$

$x_2 = 12$
$a/\rho^* = 0.96$
$C = 15.75\rho^2$

Figure 7. Single source and multiple receivers (Receivers are marked with •, source is marked with a star)

Figure 7 prompts the hypothesis that a/ρ^* approaches 1 as x_2 increases. The hypothesis turns out to be correct, as shown in the following theorem:

Theorem 1: As the number of receivers x_2 approaches infinity, the optimized area coverage approaches $C_{UB} = 18.31\rho^2$, with an optimal normalized circular radius of 1.

Proof: There are two cases, $a/\rho \le 1$ and $a/\rho > 1$ (Figure 8). For the first case, as x_2 approaches ∞, the coverage diagram becomes a circle of radius $a + \sqrt{a^2 + \rho^2}$. For $a/\rho > 1$ the diagram becomes a smaller circle of radius $a - \sqrt{a^2 - \rho^2}$, plus a ring with $a + \sqrt{a^2 + \rho^2}$ outer and $a + \sqrt{a^2 - \rho^2}$ inner radii. By simple geometric analysis the limiting C is:

$$C = \begin{cases} \pi\left(a + \sqrt{a^2 + \rho^2}\right)^2 & , a/\rho \le 1 \\ \pi\left[\left(a + \sqrt{a^2 + \rho^2}\right)^2 - \left(a + \sqrt{a^2 - \rho^2}\right)^2 + \left(a - \sqrt{a^2 - \rho^2}\right)^2\right], & a/\rho > 1 \end{cases} \tag{9}$$

It is a calculus exercise to show that the maximizing value for a/ρ is 1. Figure 9 shows that the maximum is surprisingly sharp. The optimized coverage diagram consists of lots of lemniscates, each ending at a radius of $\rho(1+\sqrt{2})$, and the limiting value for the covered area is $C_{UB} = \pi\left(\rho(1+\sqrt{2})\right)^2 = 5.82\pi\rho^2 = 18.31\rho^2$. **QED**

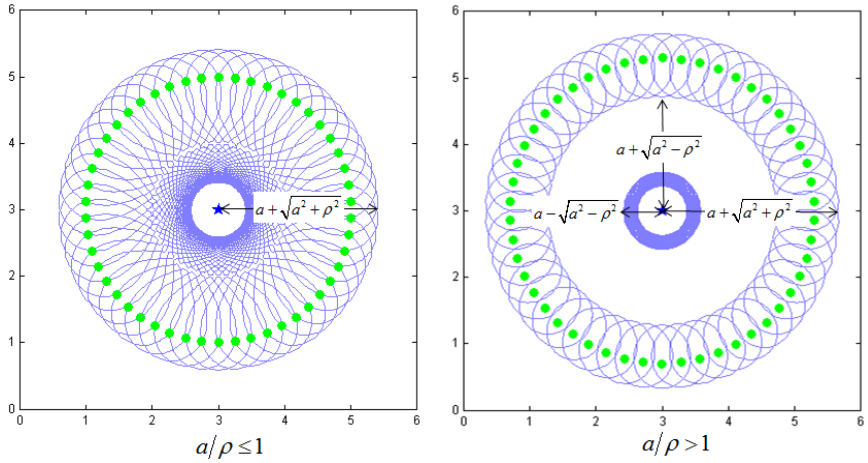

Figure 8. Circular coverage with large number of receivers (•) symmetrically placed around a single source. Left: $a/\rho \le 1$ **Right:** $a/\rho > 1$.

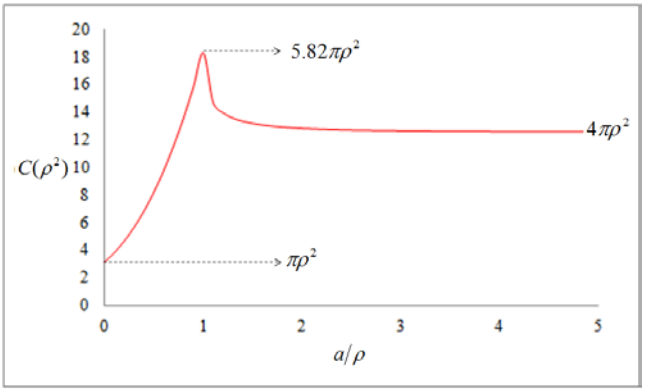

Figure 9. Coverage with many receivers placed in a circle around a single source.

Putting all receivers at the same radius from a single source cannot be the optimal configuration when the number of receivers is large because the total area coverage is bounded above by C_{UB}. Since any point in the plane can be covered by putting a receiver there, the covered area should increase without bound as the number of receivers increases. We next investigate placing the receivers in concentric, non-overlapping rings, as in Figure 10 (Left), rather than all in a single ring. We will show that this tactic results in the covered area being ultimately proportional to $\sqrt{x_2}$.

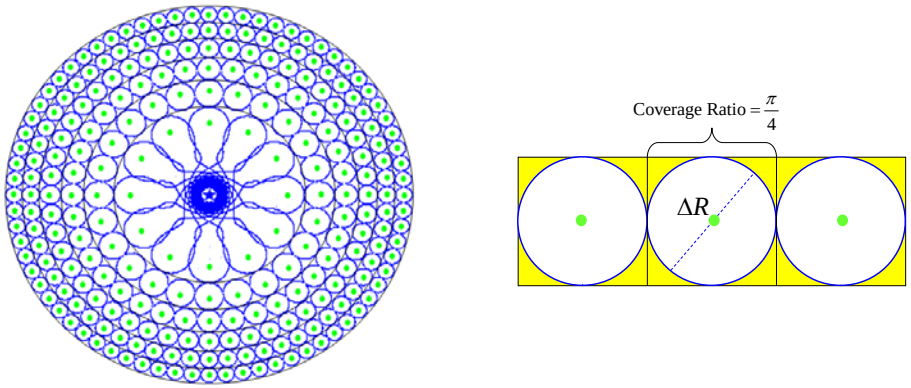

Figure 10. Left: Packing receivers (•)in rings. Right: Coverage within a ring

If R is the central radius of a large ring centered on the source, then a receiver within the ring covers a small circle with radius ρ^2/R. Therefore the width of the ring and the diameter of each receiver within the ring are both $\Delta R \equiv 2\rho^2 / R$. The number of receivers that will fit in the ring without overlap is the central circumference of the ring divided by the diameter of a receiver, $\Delta N \equiv \frac{2\pi R}{2\rho^2 / R} = \pi R^2/\rho^2$. Let $N(R)$ be the total number of receivers within the circle of radius R, including all rings within that circle. When R is large, ΔR becomes small and

$$dN(R) / dR \cong \Delta N / \Delta R = \frac{\pi R^3}{2\rho^4} \tag{10}$$

Therefore, for R greater than some large radius R_0,

$$N(R) \cong N(R_0) + \int_{R_0}^{R} \frac{dN(R)}{dR} dR = C_N + \int_0^R \frac{\pi R^3}{2\rho^4} dR = C_N + \frac{\pi R^4}{8\rho^4} \tag{11}$$

with the constant C_N accounting for the center of the covered circle where receivers are perhaps not arranged in rings, as illustrated in Figure 10 (Left). The approximation becomes exact when R is large.

Let $A(R)$ be the covered area within a circle of radius R centered on the source. The fraction of the outer rings that is covered is $\pi/4$ because the receivers are arranged within each ring without overlap (see Figure 10 (Right)). Therefore, again for large R,

$$A(R) \cong C_A + \pi R^2(\pi/4) = C_A + \pi^2 R^2/4 \tag{12}$$

Ignoring both C_N and C_A because we are only interested in large values of R,

$$A(R) = \sqrt{\pi^3 / 2}\rho^2 \sqrt{N(R)} = 3.94\rho^2 \sqrt{N(R)} \tag{13}$$

As claimed above, the covered area grows with the square root of the number of receivers.

The tactic of arranging receivers in rings suffices to demonstrate that coverage is unbounded as x_2 grows large, but it is surely not optimal. For large R, better coverage could be achieved by using additional receivers to cover gaps in small rings, even at the cost of overlap.

General pattern optimization

When there are equal numbers of sources and receivers, our exploration of the alternatives shows that equally spaced rectangular patterns achieve the highest area coverage values. Figure 11 depicts the best-known pattern, the optimal ratio a/ρ^*, and the corresponding area coverage (C) values for 2, 3, 6, and 10 pairs. In each case coverage was determined by Monte Carlo simulation. Each pattern has only a single parameter, the buoy spacing a, which was varied exhaustively to find the best coverage.

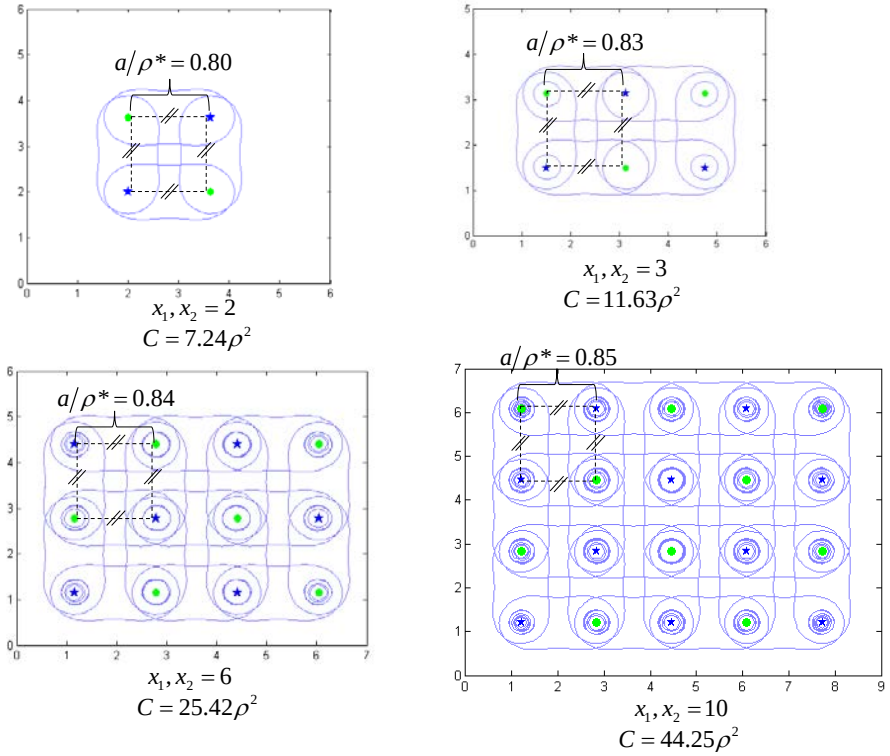

Figure 11. Coverage of equal numbers of sources and receivers deployed in rectangular patterns (Receivers are marked with •, sources are marked with a star)

Another analytic alternative for general pattern optimization is to use mathematical programming to determine the optimal locations of buoys within some fine grid that is superimposed on the region containing the target. Let the rectangular region A consist of m and n grid points in the x and y dimensions, respectively. The goal is to maximize the total number of covered grid points by optimally assigning buoys to locations in the grid.

Source i located at $\left(s_i^x, s_i^y\right)$ and receiver j located at $\left(r_j^x, r_j^y\right)$ can detect (cover) target k at grid point $\left(t_k^x, t_k^y\right)$ if the product of source-target and target-receiver distances is less than or equal to ρ^2; that is, if $\sqrt{\left[(s_i^x - t_k^x)^2 + (s_i^y - t_k^y)^2\right]\left[(r_j^x - t_k^x)^2 + (r_j^y - t_k^y)^2\right]} \le \rho^2$. Let u_{ijk} be a 0-1 (binary) variable whose value is 1 if the k^{th} grid point is covered by the i^{th} source and the j^{th} receiver, or otherwise 0. A grid point is covered if it is inside the detection region of any source-receiver pair, so z, the total number of grid points covered, is given by

$$z = \sum_{k=1}^{mn}\left(1-\prod_{i=1}^{x_1}\prod_{j=1}^{x_2}\left(1-u_{ijk}\right)\right). \qquad (14)$$

We can now formulate an integer nonlinear programming model INLP for maximizing the total number of cells covered:

$$\max z = \sum_{k=1}^{mn}\left(1-\prod_{i=1}^{x_1}\prod_{j=1}^{x_2}\left(1-u_{ijk}\right)\right)$$

Subject to

$$u_{ijk} \le \frac{\rho^4}{\left[(s_i^x - t_k^x)^2 + (s_i^y - t_k^y)^2\right]\left[(r_j^x - t_k^x)^2 + (r_j^y - t_k^y)^2\right]} \quad \forall\ i, j, k \qquad [1]$$

$$0 \le s_i^x, r_j^x \le m \quad \forall\ i, j \qquad [2]$$

$$0 \le s_i^y, r_j^y \le n \quad \forall\ i, j \qquad [3]$$

$$0 \le u_{ijk} \le 1 \quad \forall\ i, j, k \qquad [4]$$

Constraints [1] in INLP are nonlinear because they involve products of decision variables, and all variables are restricted to be integers. INLP is a difficult type of optimization for which we have found locally optimal solutions using GAMS (2005) for various values of x_1 and x_2 (see Figure 12). It can be seen that these locally optimal patterns all have some kind of welcome polygonal symmetry. While mathematical programming would become problematic for large problem instances, it does give plausible results for small numbers of buoys, as well as insight into optimal arrangements of large patterns.

How much is to be gained by using patterns that are carefully designed, rather than random? Figure 13 provides a partial answer using equation (7) to measure the effectiveness of a random field. The bars represent the actual optimal and random coverages for selected x_1 and x_2 values and the line above the bars expresses the coverage gain as a percentage. The minimum gain in area coverage is 38% for the 1x2 case and maximum is 81% for the 1x12 case. It should be apparent that randomness is not a property to be sought tactically, but only a conservative assumption that enables simple analysis. This is similar to the development of the Random Search Formula (Koopman, 1956).

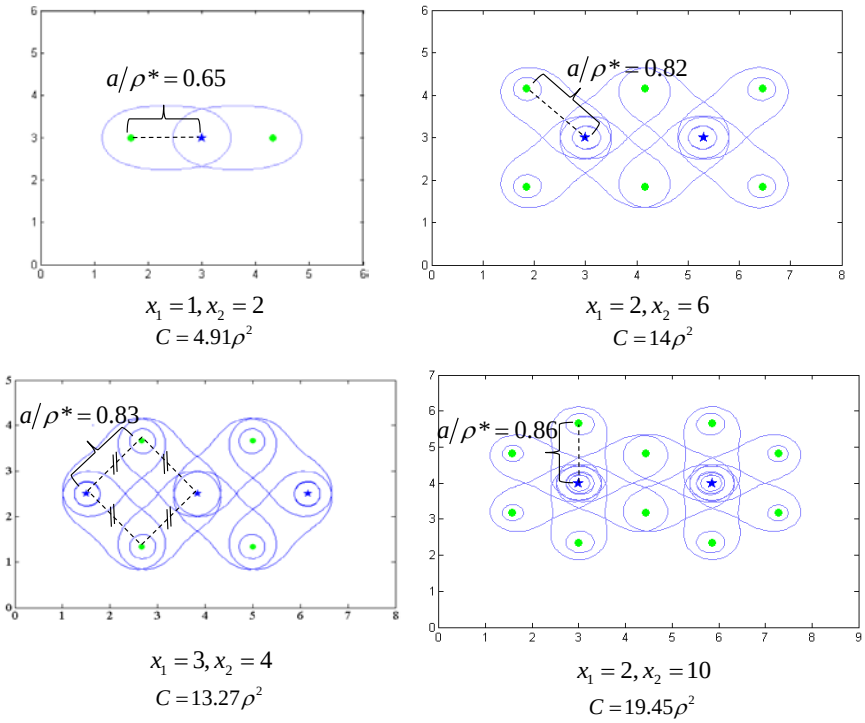

Figure 12. Locally optimal GAMS solutions for various multistatic systems (Receivers are marked with • , sources are marked with a star)

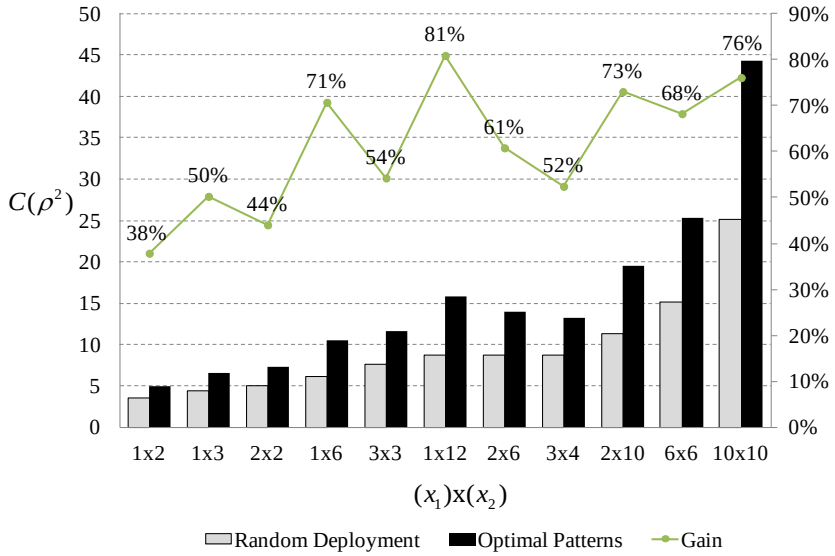

Figure 13. Gain achieved by optimal patterns vs random deployment

MOBILE SOURCE AND STATIONARY RECEIVERS

The coverage and tracking performance of a multistatic system can be improved by using a mobile source (Tharmarasa, et al, 2009). In this section we assume that our multistatic system consists of a source moving on a straight line through an infinite Poisson field of stationary receivers of density *h*. A practical scenario for such a system

would be a maritime surveillance or anti-submarine warfare situation where a continuously emitting surface ship (possibly the towed-array low-frequency active sonar (LFAS) proposed by Coraluppi & Grimmett, (2004)) uses a field of stationary receivers to search for objects such as mines, wrecks or hostile submarines.

Figure 14 shows the region covered by such a moving sensor. Each receiver is surrounded by a covered circle that gets smaller for receivers that are located far from the track of the source. Roughly speaking, targets near the source's track will be detected.

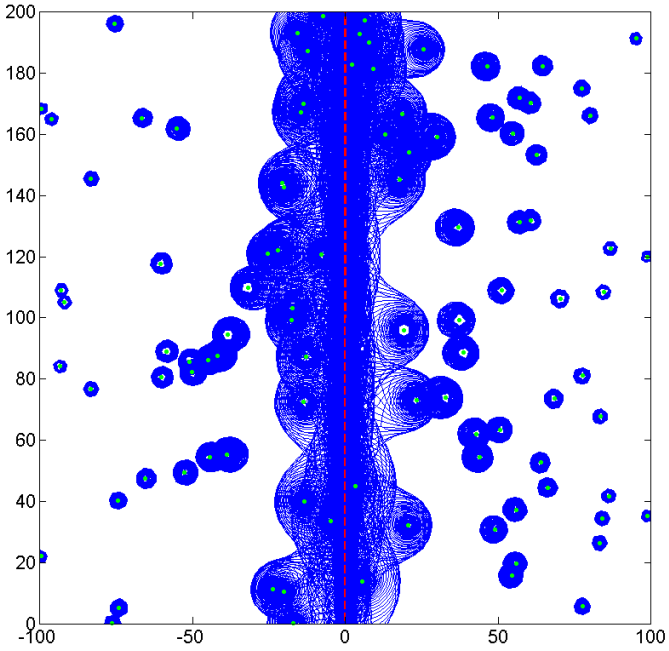

Figure 14. Coverage of a moving source in a random field of stationary receivers (Receivers are marked with • , source moves along the dashed line)

For analytical purposes, suppose that the source moves along the *y*-axis, as partially shown in Figure 14, and consider a target at $(0, x)$. The probability of detection when the source is at the origin is the probability that there is at least one receiver in a circle centered on the target with radius ρ^2/x. In a Poisson field of receivers, that probability is

$$P(x) = 1 - \exp(-\frac{\pi h \rho^4}{x^2}) \tag{15}$$

$P(x)$ is also the probability of detection as the source moves over the whole *y*-axis because the closest distance from source to target is $|x|$; the target will never be detected if it is not detected at the closest point of approach. Therefore (15) is a lateral range curve (Koopman, 1956). For ρ =1, the lateral range curve for h=0.2, 0.4 and 0.6 is shown in Figure 15.

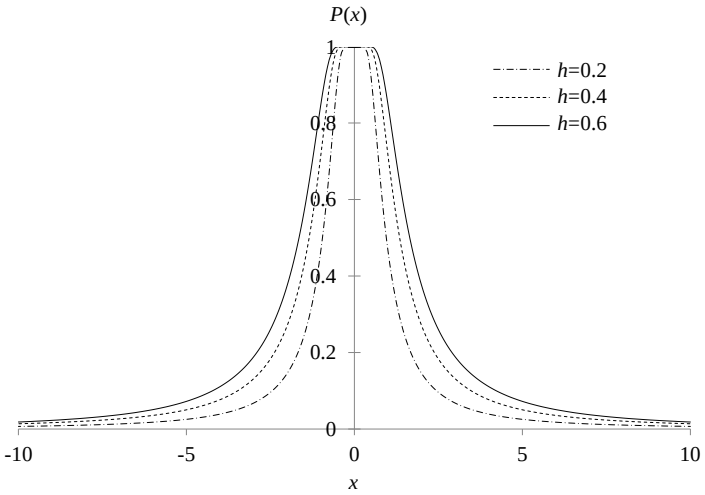

Figure 15. Lateral range curves for various receiver densities

It happens that (15) has the same analytic form as the lateral range curve of an inverse cube law sensor (Koopman, 1956), so some of the analytic results that apply to such sensors are also valid here. In particular, since sweep width *W* is the area under the lateral range curve,

$$W = \int_{-\infty}^{\infty} P(x)dx = 2\int_{0}^{\infty}\left(1-\exp(-\frac{\pi h\rho^4}{x^2})\right)dx = ... = 2\pi\rho^2\sqrt{h}\,. \tag{16}$$

We see in (16) a strong motivation for sparse fields of high quality receivers. For example, if one can double ρ by utilizing only ¼ as many receivers, the sweep width will double.

Another known property of inverse cube law sensors (Koopman, 1956) is the probability of detection $Q_{ind}(S)$ if parallel sweeps are spaced *S* apart in an infinite grid, with the target being located randomly with respect to the grid. This probability is

$$Q_{ind}(S) = erf\left(\frac{\sqrt{\pi}}{2}\frac{W}{S}\right), \tag{17}$$

where *erf*() is the error function. Lying behind (17) is an assumption that all parallel sweeps are independent, which is not true in the multistatic case because the Poisson field of receivers is the same for all sweeps. Let $Q(S)$ be the corresponding probability for the multistatic case. To evaluate $Q(S)$, we need to consider only the sweep that is closest to the target, with the exact location of the target being uniformly distributed in the interval $[-S/2, S/2]$. Using (15) and (16) the average probability of detection is

$$Q(S) = \frac{2}{S}\int_{0}^{S/2}\left[1-\exp\left(-\left(\frac{W}{2\sqrt{\pi}x}\right)^2\right)\right]dx\,. \tag{18}$$

Letting $u \equiv 2x/S$ and $y \equiv W/S$, (18) becomes

$$Q(S) = F(y) \equiv \int_{0}^{1}\left[1-\exp\left(-\frac{y^2}{\pi u^2}\right)\right]du\,. \tag{19}$$

Change the variable of integration to $v = y^2/(\pi u^2)$, so that

$$Q(S) = -\pi^{-0.5} y \int_{\infty}^{y^2/\pi} (1-\exp(-v))(0.5v^{-1.5})dv = \pi^{-0.5} y \int_{y^2/\pi}^{\infty} (1-\exp(-v))(0.5v^{-1.5})dv . \quad (20)$$

We now employ integration by parts. Equation (21) below is true because the integral is a perfect differential.

$$\pi^{-0.5} y \int_{y^2/\pi}^{\infty} d\,/\,dv\{(1-\exp(-v))(-v^{-0.5})\}dv = (1-\exp(-y^2/\pi)) . \quad (21)$$

Performing the indicated derivative, we find that one of the two terms is $Q(S)$, so

$$Q(S) = 1-\exp(-y^2/\pi) + \pi^{-0.5} y \int_{y^2/\pi}^{\infty} \exp(-v)v^{-0.5}dv . \quad (22)$$

The Gamma distribution with parameter α set to 1 is $G(x) \equiv \pi^{-0.5}\int_0^x \exp(-v)v^{-0.5}dv$, a standard statistical distribution. Since $G(\infty) = 1$, we can rewrite (22) as

$$Q(S) = 1-\exp(-y^2/\pi) + y(1-G(y^2/\pi)) . \quad (23)$$

Equation (23) is our final expression for the probability of detection when a moving source repeatedly sweeps a Poisson field of stationary receivers with tracks spaced S apart. If the receiver locations were all independently sampled for each track, we would instead find the detection probability to be the same as in the inverse cube law case. Figure 16 compares the dependent (23) and independent (17) cases. It can be seen that the inverse cube law provides an optimistic assessment of detection probability for dependent multistatic sweeps.

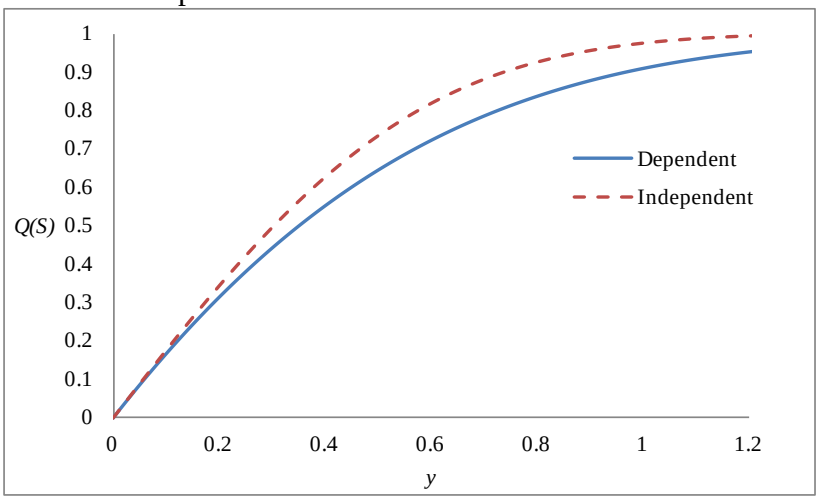

Figure 16. Detection probability versus *y=W/S* for dependent and independent (inverse cube law) parallel tracks

COST/EFFECTIVENESS

In addition to finding the best balance between sources and receivers, a study of cost/effectiveness should include evaluation of the co-location option. There are some good arguments, tactical convenience being one of them, for deploying buoys in "posts"

that consist of co-located sources and receivers. Cox (1989, p. 23), in response to a question about his seminal multistatic work, stated that "It makes sense to me to use multiple receivers with a single high powered source. One of these should be monostatic so that $TL_1 = TL_2$. The others are bistatic and provide increased coverage and countermeasure resistance". Sonobuoy fields of this type will be called PR (Post/Receiver) fields. One of our objects is to compare the effectiveness of PR fields with that of the SR (Source/Receiver) fields that were considered earlier. PR fields have no independent sources, whereas SR fields have no posts. For analytic tractability in this section we again assume that all buoys are located at random in Poisson fields.

If any post in a PR field is closer to the target than ρ, then the miss probability is zero. Otherwise the same logic that underlies (2) applies, so the formula for miss probability in a PR field is similar to (2). If s is the dimensionless density of posts and t is the dimensionless density of independent receivers, then the miss probability is $Q(s,st)$, where

$$Q(s,v) = \int_s^\infty \exp(-(\frac{v}{x} + x))dx\,. \tag{24}$$

The analytic effect of changing sources into posts is evidently to change the lower limit of the integral from 0 in (2) to s in (24), thus decreasing the miss probability. If there are no independent receivers ($t = 0$), the miss probability according to (24) is now $\exp(-s)$ instead of 1. Except for that special case, there seems to be no way to express (24) in terms of commonly available functions.

Formula (24) assumes that the buoys are spread out in a constant density over the whole plane. If x_1 posts and x_2 independent receivers are spread out randomly over a large area A, then we can estimate the detection probability within A by making the neutrality assumption and substituting $s = \pi\rho^2 x_1 / A$ and $t = \pi\rho^2 x_2 / A$, as in the earlier section on randomly placed fields. We can then consider the question of how a given budget should be divided between sources and receivers, as well as the question of whether PR fields are superior to SR fields.

First, consider the SR case. If sources and receivers cost c_1 and c_2 each, the cost of a buoy field consisting of x_1 sources and x_2 receivers is $c_1 x_1 + c_2 x_2$. The detection probability is determined by the product $x_1 x_2$, so it is a calculus exercise to conclude that sources and receivers should each consume half of the available budget. If the budget is B, the resulting product is $x_1 x_2 = \frac{B^2}{4c_1 c_2}$. Substituting this into (7), we find that $C = (0.4)\frac{\pi\rho^2 B}{\sqrt{c_1 c_2}}$. If A is the area to be covered, we can also compute the dimensionless effort density $y = \frac{\pi\rho^2 B}{A\sqrt{c_1 c_2}}$. Given y, detection probability can be computed using (3), or possibly (6) if buoy concentration is considered.

In the special case where $c_1 = c_2$, the number of sources in an SR field should equal the number of receivers. If we were instead to deploy a PR field consisting purely of posts that cost $2c_1$ each, then each post would cover an area of $\pi\rho^2$ and the total area

covered would be $\frac{\pi\rho^2 B}{2c_1}$. This exceeds the SR area coverage by 20%, so we have at least one situation where a PR field is preferred to an SR field. A PR field might be even more effective if it included some independent receivers, a possibility that we consider next.

Subsequent investigations in this section are based on the dimensionless buoy densities $s = \pi\rho^2 x_1 / A$ and $t = \pi\rho^2 x_2 / A$. We impose the cost constraint $s + ct \le b$, where $c \equiv c_2 / c_1$ and $b \equiv \frac{\pi B \rho^2}{c_1 A}$. There is no loss of generality in restricting the coefficient of *s* to be 1, since this is just a choice of monetary unit. We can summarize the optimal balance between sources and receivers in an SR field by

$$s = \frac{b}{2}, \quad t = \frac{b}{2c}, \quad st = \frac{b^2}{4c}, \text{ and } y = 2\sqrt{st} = \frac{b}{\sqrt{c}}. \tag{25}$$

In a PR field, if the cost of each post is the sum of the costs of one source and one receiver, then the proper cost constraint is $(1+c)s + ct \le b$. Let $Q_{min}(b,c)$ be the result of minimizing *Q*(*s*,*st*) subject to that constraint. For sufficiently small budgets, the result of this minimization will be that *t* = 0; that is, no independent receivers should be utilized. To prove this, let $Q_1(s,t)$ and $Q_2(s,t)$ be the derivatives of *Q*(*s*,*st*) with respect to *s* and *t*, respectively, and define the function

$$H(s,t) = s\int_s^\infty \exp(-(x + \frac{st}{x}))\frac{dx}{x}. \tag{26}$$

Then $Q_2(s,t) = -H(s,t)$ and $Q_1(s,t) = -\frac{t}{s}H(s,t) - \exp(-(s+t))$. For (*s*,0) to be minimizing, it is necessary that there exist a Lagrange multiplier λ such that (*s*,0) minimizes the expression $Q(s,st) + \lambda(s(1+c) + tc)$, while simultaneously $s = b/(1+c)$. The first-order minimization conditions are that $Q_1(s,0) + \lambda(1+c) = 0$ and $Q_2(s,0) + \lambda c \ge 0$. Since $Q_1(s,0) = -\exp(-s)$, the first equation requires $\lambda = \exp(-s)/(1+c)$. Substituting this into the inequality, we must have $\exp(s)H(s,0) \le c/(1+c)$. Let *H*(*s*) be the left-hand side of this inequality. Then

$$H(s) = s\exp(s)\int_s^\infty \exp(-x)\frac{dx}{x} = s\exp(s)\left[\int_0^s \frac{1-\exp(-u)}{u}du - \ln(s) - \gamma\right], \tag{27}$$

where γ is Euler's constant (0.577 …). Figure 17 shows this function as evaluated by numerically integrating the right-hand-side of (27).

If the budget is *b*, and if *H*(*b*/(1+*c*)) is smaller than the cost ratio *c*/(1+*c*), as it will be if *b* is sufficiently small, then the best PR field will spend the entire budget on posts. These posts should be spread over all of *A* because posts are effectively monostatic sonobuoys. The resulting miss probability will be $Q(s,0) = \exp(-b/(1+c))$. However, it is still possible that an SR field might be better than even the best PR field. The maximum possible value of *y* is given by (25) and the corresponding SR detection probability by (6), so the overall minimal miss probability, considering both the PR and SR types, will be

$$Q_{\min}(b,c) = \min\left\{\exp(-\frac{b}{1+c}), 1 - PD*(\frac{b}{\sqrt{c}})\right\}, \text{ for small } b \qquad (28)$$

For very small budgets, the PR miss probability is approximately $1-b/(1+c)$ and the SR miss probability is approximately $1-0.4b/\sqrt{c}$. Both expressions are linear in *b*, so it is easily shown that the PR field is preferred for such budgets if and only if $0.25 < c < 4$.

Example: Consider the case (*b*,*c*) = (1,1). Since $H(0.5) = 0.461$, which is smaller than 0.5, the best PR field will have no independent receivers. However, the second term in (28) is minimizing when $b = 1$, so the overall best field is actually of type SR, achieving its detection probability of 0.4 by slightly concentrating the buoys in part of *A*. If *b* is reduced to 0.1 while *c* remains 1, the best PR field will still contain only posts, but now will be preferred to the SR field. The PR field will also be preferred for any budget smaller than 0.1.

Example: Suppose $c = 1/5$, the approximate ratio of SSQ-53 to SSQ-125 sonobuoys. Because *c* is not in the required interval, SR will be preferred to PR for very small budgets, with the buoys deployed in a small part of *A*. A numerical investigation reveals that SR is preferred to PR for all budgets when $c = 1/5$.

Both of the above examples are consistent with the claim that the most cost/effective field will never include all three of independent sources, independent receivers, and posts. As long as receivers are cheaper than sources, this means that an optimal field will always be either a PR field with no independent sources or an SR field with no posts. If that claim is true, then (28) is correct for all values of (b,c), not just when *b* is small. After extensive but not exhaustive experimentation (see Washburn (2010)), we have found no exceptions to the claim. Using different measures of effectiveness, Ozols & Fewell (2011) also find no exceptions.

It is worth noting that, if a constant *K* is added to both c_1 and c_2 in the analyses above, the effect will be significant and favor PR fields over SR fields. If *K* represents a delivery cost that applies to all sonobuoys, one could even argue that the cost of a post should be only $c_1 + c_2 + K$, rather than $c_1 + c_2 + 2K$, which would further favor PR fields.

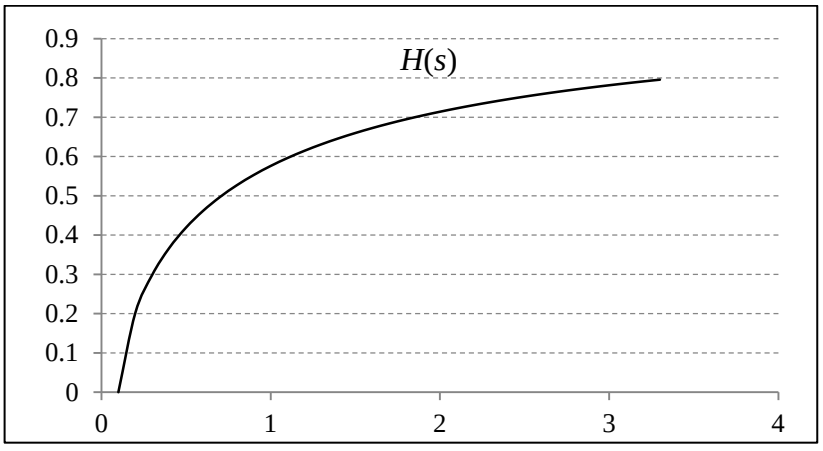

Figure 17. The function *H*(*s*) is continuous, concave, and increasing, with *H*(0)=0.

RELIABILITY AND DIRECT BLAST

The idea that detection is merely a matter of being close enough to the target underlies all of the above calculations, but is only approximately true in the real world. One reason for this is that some buoys may not function correctly, in which case their distances from the target are immaterial. This possibility is easily handled theoretically in SR fields. If r_s and r_r are the reliabilities of sources and receivers, it is simply a matter of replacing the dimensionless densities s and t by sr_s and tr_r, respectively. This is because Poisson fields "thinned" in this manner remain Poisson fields. A similar argument will not work for PR fields because a post might get effectively turned into an independent source should its receiver not function.

Proximity might not be sufficient even when all buoys function as intended. In multistatic sonar systems, receivers hear the transmitted signal directly, in addition to the signal reflected from the target. This "direct blast" is actually necessary for locating the target because the difference in time between the direct and reflected signals establishes an ellipse upon which the target must lie. However, the direct blast is much stronger than the reflected signal, and may completely obscure it if the time difference in arrivals is small enough. The principal situation where this happens is when the target is more or less directly between the source and the receiver. A simple approximation of the effect is the "dead zone" shown in Figure 18, where receivers will not detect the target because of the direct blast arriving nearly simultaneously. The angle $\pi - \theta$ measures the extent of the pie-shaped dead zone, with $\theta = \pi$ corresponding to no dead zone at all.

It is not difficult to include the effect of dead zones in a Monte Carlo simulation that begins by simulating the locations of the target, the sources and the receivers. For each source/receiver pair that passes the proximity test for a specific target, one simply checks whether the receiver is in the dead zone of the source, declaring the detection attempt to be a failure if so. The resulting simulation is only slightly more complicated than one without dead zones. Unfortunately, however, this simplicity does not extend to analytic attempts to find a generalization of (3). We are not aware of any exact formulas for detection probability, but the following theorems at least offer lower bounds.

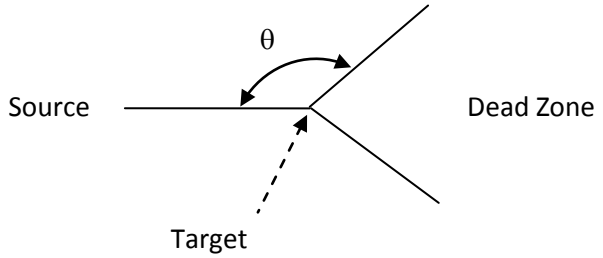

Figure 18. Illustrating a dead zone where receivers are useless on account of direct blast.

Theorem 2: In an SR field, let s and t be the dimensionless densities of sources and receivers, respectively, as in the section on randomly placed fields, but add the requirement that the receiver buoy in a successful pair must not be in the dead zone of its source. Let $p \equiv \theta / \pi$, and let $y = 2\sqrt{pst}$. If y is substituted into (3) one has a lower bound on the detection probability.

Proof: Let E be the event that the target is detected by the source that is closest to

it. *E* will happen if and only if there is at least one eligible receiver that is sufficiently close to the target; a receiver being "eligible" if and only if it is not in the dead zone of the closest source. The probability that any independent receiver is eligible is *p*, so eligible receivers are a Poisson field with dimensionless density *pt*. To calculate *P*(*E*), we can now proceed as in the derivation of (3), except that *pt* needs to substituted for *t*. The effect of this is that *y* is modified as in the statement of the theorem, and $P(E) = 1 - yK_1(y)$. This is a lower bound on the detection probability because it is possible for the target to be detected even when the closest source fails. **QED**

Theorem 3: In a PR field, let *s* and *t* be the dimensionless densities of posts and receivers, respectively, but add the requirement that the receiver buoy in a successful pair must not be in the dead zone of its source. Let $p \equiv \theta / \pi$. Then $1 - Q(s, pst)$ is a lower bound on detection probability, where *Q*( ) is the function defined in (24).

Proof: If the post that is nearest to the target is closer than ρ, then detection is certain because a post's own receiver cannot be in a dead zone. Let *E* be the event that the nearest post is farther away than ρ, but nonetheless detects the target through some other eligible independent receiver. *E* will happen if and only if there is at least one such receiver that is sufficiently close to the target. The probability that any independent receiver is eligible is *p*, so eligible receivers are a Poisson field with dimensionless density *pt*. To calculate *P*(*E*), we can now proceed as in the derivation of (24), except that *pt* needs to substituted for *t*. The result of this is as stated in the theorem. This is a lower bound on the detection probability because it is possible for the target to be detected even when the closest post fails. **QED**

Simulation experiments confirm Theorem 3, with the pessimism of the lower bound increasing as θ becomes smaller. Presumably the increasing pessimism is because sources other than the closest become more important as the direct blast effect becomes stronger. When $\theta = 3\pi / 4$, the theoretical formula is about 5% pessimistic. See Washburn (2010) for further detail.

SUMMARY

We have developed several formulas for the effects of multistatic sensor fields, both for static fields (formulas (6) and (7)) and for mobile sources moving through a field of static receivers (formula (23)). Most formulas depend on the assumption that receivers are randomly located, but experiments show that carefully designed patterns offer a significant improvement. Cost-effectiveness analysis reveals that multistatic fields are best when sources and receivers have significantly different costs. When the costs are nearly equal, monostatic fields consisting entirely of posts should also be considered.

LIST OF REFERENCES

Abramovitz, S., and Stegun, I. 1964. *Handbook of mathematical functions*. Applied Mathematics Series 55. Washington, D.C.: National Bureau of Standards, 374-8.

Amanipour, V., and Olfat, A. 2011. CFAR Detection for Multistatic Radar, *Signal Processing*, 91(1), 28-37.

Ammari, H., Garnier, J., Kang, H., Lim, M., and Sølna, K. 2012. Multistatic Imaging of Extended Targets, *SIAM Journal on Imaging Sciences*, 5(2), 564-600.

Bowen, J., and Mitnick, R. 1999. A Multistatic Performance Prediction Methodology, *Johns Hopkins Apl Technical Digest*, *20*(3).

Bradaric, I., Capraro, G. T., Weiner, D. D., and Wicks, M. C. 2006. Multistatic Radar Systems Signal Processing, IEEE Conference on Radar, pp. 8.

Chacko G. and DelBalzo D.R. 2007. Tactical Planning with Genetic Algorithms for Multistatic Active Sonobuoy Systems, Proceedings of 19th International Congress on Acoustics, Madrid.

Coon, A. 1997. Spatial Correlation of Detections For Impulsive Echo Ranging Sonar. *Johns Hopkins Apl Technical Digest*, *18*(1), pp. 105-112. Accesssed in 2010 from http://www.jhuapl.edu/techdigest/td1801/coon.pdf .

Coraluppi, S., and Grimmett, D. 2004. Intra-Ping Timing Issues in Multistatic Sonar Tracking. Proceedings of the 7th International Conference on Information Fusion.

Coraluppi, S. 2005. Distributed Tracking in Multistatic Sonar. IEEE Transactions on *Aerospace and Electronic Systems*, Volume: 41, Issue: 3, pp. 1138-1147.

Cox, H. 1989. Fundamentals of Bistatic Active Sonar. In Y. Chan (Ed.), *Underwater acoustic data processing*, Kluwer, pp. 3-24.

Daun, M., Nickel, U., and Koch, W. 2012. Tracking in Multistatic Passive Radar Systems Using DAB/DVB-T Illumination, *Signal Processing*, 92(6), pp. 1365-1386.

Devaney, A. J. 2005. Time Reversal Imaging of Obscured Targets from Multistatic Data, *IEEE Transactions on Antennas and Propagation*, 53(5), pp. 1600-1610.

Feller, W. 1950. *An introduction to probability theory and its applications*, p. 149, Wiley.

GAMS Development Corporation, General algebraic modeling system (GAMS). 2005. Retrieved December 15, 2007, http://www.gams.com.

Gong, X., Zhang, J., Cochran, D., and Xing, K. 2013. Barrier Coverage in Bistatic Radar Sensor Networks: Cassini Oval Sensing and Optimal Placement. Proceedings of the 14th ACM International Symposium on Mobile Ad Hoc Networking and Computing, pp. 49-58.

Koopman, B. 1956. *Search and Screening*, Operations Evaluation Group Report 56, Chief of Naval Operations, Washington, DC, chapter 2.

Krieger, G., Fiedler, H., Mittermayer, J., Papathanassiou, K., and Moreira, A. 2003. Analysis of Multistatic Configurations for Spaceborne SAR Interferometry. IEE Proceedings-Radar, Sonar and Navigation, 150(3), pp. 87-96.

Krout, D. W., Fox, W. L., and El-Sharkawi, M. A. 2009. Probability of Target Presence for Multistatic Sonar Ping Sequencing. *IEEE Journal of Oceanic Engineering*, 34(4), 603-609.

Martina, D., and Frank, E. 2010. Tracking Algorithms for Multistatic Sonar Systems. *EURASIP Journal on Advances in Signal Processing*, vol. 2010.

Ozols, S and Fewell, M.P. 2011. On the Design of Multistatic Sonobuoy Fields for Area Search, Defence Science and Technology Organization, DSTO-TR-2563, Edinburgh, Australia.

Ozols, S., Fewell, M.P. and Thredgold, J.M. 2011. Track-Initiation Probability for Multistatic Sonar Fields, Technical report, ADA554481.

Paolini, E., Giorgetti, A., Chiani, M., Minutolo, R., and Montanari, M. 2008. Localization Capability of Cooperative Anti-Intruder Radar Systems. *EURASIP Journal on Advances in Signal Processing*, 2008(17).

Saksena, A., and Wang, I. J. 2008. Dynamic Ping Optimization for Surveillance in Multistatic Sonar Buoy Networks with Energy Constraints, 47th IEEE Conference on Decision and Control, pp. 1109-1114.

Signal Online. 2012. http://www.afcea.org/content/?q=taxonomy/term/1258, AFCEA, accessed in 2014.

Simakov, S. 2008. Localization in Airborne Multistatic Sonars, *IEEE Journal of Oceanic Engineering*, 33(3), pp. 278-288.

Stinco, P., Greco, M. S., Gini, F., and Farina, A. 2013. Posterior Cramér–Rao Lower Bounds for Passive Bistatic Radar Tracking with Uncertain Target Measurements. *Signal Processing*, 93(12), pp. 3528-3540.

Tharmarasa, R., Kirubarajan, T., and Lang, T. 2009. Joint Path Planning and Sensor Subset Selection for Multistatic Sensor Networks, IEEE Symposium on

Computational Intelligence for Security and Defense Applications, pp. 1-8.

USN, 2014 Department of the Navy Fiscal Year 2015 Budget Estimates, http://www.finance.hq.navy.mil/fmb/15pres/OPN_BA3_BOOK.pdf, Justification Book, Vol: 3, exhibit P-5, accessed in 2014.

Wang, L., Cheney, M., and Borden, B. 2012. Multistatic Radar Imaging of Moving Targets, *IEEE Transactions on Aerospace and Electronic Systems*, 48(1), pp. 230-242.

Wathelet, A., Strode, C., Vermeij, A., and Been, R. 2008. Optimisation in the Multistatic Tactical Planning Aid (MSTPA), NURC report NURC-FR-2008-013, La Spezia, Italy.

Washburn, A. R. 2010. A Multistatic Sonobuoy Theory, Naval Postgraduate School report NPS-OR-10-005, Monterey, CA.

Xie, Y., Guo, B., Xu, L., Li, J., and Stoica, P. 2006. Multistatic Adaptive Microwave Imaging for Early Breast Cancer Detection. IEEE Transactions on Biomedical Engineering, 53(8), pp. 1647.